THE JOURNAL OF BIOLOGICAL CHEMISTRY
Vol. 276, No. 41, Issue of October 12, pp. 38224–38230, 2001
Printed in U.S.A.

Nuclear Retention of ATM at Sites of DNA Double Strand Breaks*

Received for publication, April 4, 2001, and in revised form, July 9, 2001
Published, JBC Papers in Press, July 13, 2001, DOI 10.1074/jbc.M102986200

Yair Andegeko, Lilach Moyal, Leonid Mittelman‡, Ilan Tsarfaty§, Yosef Shiloh¶, and Galit Rotman

From the David and Inez Myers Laboratory for Genetic Research, Department of Human Genetics and Molecular Medicine, ‡Interdepartmental Core Facility, and §Department of Human Microbiology, Sackler School of Medicine, Tel Aviv University, Ramat Aviv 69978, Israel

The ATM protein kinase mediates a rapid induction of cellular responses to DNA double strand breaks (DSBs). ATM kinase activity is enhanced immediately after exposure of cells to DSB-inducing agents, but no changes in its amount or subcellular location following that activation have been reported. We speculated that some of the ATM molecules associate with sites of DSBs, while the rest of the nuclear ATM pool remains in the nucleoplasm, masking detection of the damage-associated ATM fraction. Using detergent extraction to remove nucleoplasmic proteins, we show here that immediately following induction of DSBs, a fraction of the ATM pool becomes resistant to extraction and is detected in nuclear aggregates. Colocalization of the retained ATM with the phosphorylated form of histone H2AX (γ-H2AX) and with foci of the Nbs1 protein suggests that ATM associates with sites of DSBs. The striking correlation between the appearance of retained ATM and of γ-H2AX, and the rapid association of a fraction of ATM with γ-H2AX foci, are consistent with a major role for ATM in the early detection of DSBs and subsequent induction of cellular responses.

ATM is a serine/threonine protein kinase that is located mainly in the cell nucleus. Upon infliction of DNA double strand breaks (DSBs),[1] ATM mediates the rapid induction of numerous cellular responses that lead to damage repair, and activation of cell cycle checkpoints and other survival pathways (reviewed in Refs. 1 and 2).

The *ATM* gene is mutated in ataxia-telangiectasia, a pleiotropic autosomal recessive disorder characterized by progressive cerebellar degeneration, oculocutaneous telangiectasia, immunodeficiency, cancer predisposition, and an extreme sensitivity to ionizing radiation (IR). Cells derived from ataxia-telangiectasia patients exhibit chromosomal instability and a profound defect in all cellular responses to DSBs (reviewed in Refs. 3 and 4).

ATM exerts control over several signaling pathways by phosphorylating key players in an intricate network of proteins (2, 5). Prominent examples of such substrates are the p53 protein, which mediates the G_1/S checkpoint and repair processes; its inhibitor, Mdm2; the checkpoint kinase Chk2, which phosphorylates p53, Cdc25C, and Brca1, exerting control on the G_1/S and G_2/M checkpoints; and the Nbs1 protein, a component of the Mre11-Rad50-Nbs1 complex, which is involved in DSB repair and the activation of the S-phase checkpoint (5–8).

ATM kinase activity is enhanced immediately after exposure of cells to DSB-inducing agents, such as IR (9), the radiomimetic drug neocarzinostatin (NCS) (10), or etoposide (a topoisomerase II inhibitor).[2] Previous studies based on biochemical and immunofluorescence analysis suggested that activation of ATM is not accompanied by a change in its abundance or subcellular distribution (11–14). Furthermore, the amount of ATM and its activity do not vary during the cell cycle (14, 15). ATM was shown to associate with the chromatin and the nuclear matrix (14); however, in that study the association was not altered following cellular exposure to IR. In addition, ATM was shown to bind DNA ends *in vitro* (16, 17), but the *in vivo* implications of this finding remain unclear.

ATM appears to play a critical role in the surveillance and/or early detection of DSBs but is probably not directly involved in the actual repair process (2, 5). Thus, it is conceivable that only a fraction of ATM associates with sites of damage, while the remaining ATM molecules remain unbound and mask detection of the damage-associated fraction. In order to test this hypothesis, we designed a stepwise detergent extraction protocol aimed at fractionating ATM molecules according to their resistance to such extraction. Immunoblot analysis of these fractions showed that the majority of ATM was readily extracted. However, following exposure of the cells to DSB-inducing agents, a substantial fraction of the ATM pool was converted to a less extractable form within minutes after damage infliction. Immunostaining of cells extracted *in situ* showed that the extraction-resistant ATM was retained in nuclear aggregates. Colocalization of some of the retained ATM with foci of two proteins previously shown to occur at sites of DSBs, Nbs1 (18, 19), and the phosphorylated form of histone H2AX, γ-H2AX (20), point to the association of retained ATM with DSBs. The intensity and abundance of ATM aggregates and γ-H2AX foci increased with the levels of DNA damage, at a highly significant correlation. A striking correlation was also observed between the rate of appearance and dissolution of the two, suggesting a tight linkage between ATM retention and H2AX phosphorylation.

EXPERIMENTAL PROCEDURES

Cell Culture and Treatments—HeLa cells were maintained in Dulbecco's modified Eagle's medium supplemented with 10% fetal bovine serum. Human lymphoblasts (C3ABR; a gift from M. Lavin) were grown

* This work was supported by research grants from the Ataxia-Telangiectasia Medical Research Foundation, the A-T Children's Project, and the Thomas Appeal and by National Institutes of Health Grant RO1 NS 31763. The costs of publication of this article were defrayed in part by the payment of page charges. This article must therefore be hereby marked "*advertisement*" in accordance with 18 U.S.C. Section 1734 solely to indicate this fact.

¶ To whom correspondence should be addressed. Tel.: 972-3-6409760; Fax: 972-3-6407471; E-mail: yossih@post.tau.ac.il.

[1] The abbreviations used are: DSB, double strand breaks; IR, ionizing radiation; NCS, neocarzinostatin; PBS, phosphate-buffered saline; PAGE, polyacrylamide gel electrophoresis; CLSM, confocal laser-scanning microscope; PPA, percentage of positive area.

[2] T. Uziel *et al.*, unpublished results.

in RPMI with 10% fetal bovine serum. All cells were grown in a humidified atmosphere, at 37 °C with 5% CO_2. Exponentially growing cells were either mock-treated or treated with 10 grays of IR, 50 J/m^2 of UVB light, 50 μM etoposide, or NCS (at the specified concentrations). Cells were left to recover at 37 °C and harvested at the indicated time points.

Antibodies—The ATM-specific monoclonal antibody MAT3–4G10/8 was raised in mice according to standard procedures, against a synthetic peptide spanning amino acids 1967–1988 of murine Atm. This antibody recognizes both murine and human ATM and was used for immunoblot analysis. Immunofluorescence of ATM was carried out with the mouse monoclonal antibody 5C2 (a gift from E. Lee (University of Texas Health Science Center, San Antonio, TX). A rabbit polyclonal antibody against Nbs1 (Ab-1; Oncogene Research Products, Cambridge, MA), was used for immunoblotting and immunofluorescence. A rabbit polyclonal Chk2-specific antibody was a gift from S. Elledge (Baylor College of Medicine, Houston, TX). The rabbit polyclonal antibody recognizing γ-H2AX was a gift from W. Bonner (National Institutes of Health, Bethesda, MD). Secondary antibodies for Western analysis, peroxidase-conjugated goat anti-rabbit or anti-mouse, were obtained from Jackson ImmunoResearch Laboratories (West Grove, PA). Secondary antibodies for immunofluorescence analysis were goat anti-mouse-conjugated to Alexa Fluor 488 (Molecular Probes, Inc.) or donkey anti-rabbit conjugated to rhodamine (Jackson Immuno Research Laboratories).

Biochemical Fractionation and Immunoblotting—Treated or mock-treated cells were washed twice with ice-cold PBS, and cell fractionation was carried out by four consecutive extractions with increasing detergent concentration. The clarified supernatant was collected at each step and labeled as fractions I–IV. Pellets of about 10^7 cells were first resuspended for 5 min on ice in 150 μl of fractionation buffer (50 mM Hepes, pH 7.5, 150 mM NaCl, 1 mM EDTA) containing 0.2% Nonidet P-40 (Nonidet P-40), supplemented with protease inhibitors (5 μg/ml each pepstatin, leupeptin, and aprotonin) and phosphatase inhibitors (10 mM NaF, 10 mM β-glycerophosphate, 1 mM sodium orthovanadate, and 20 nM microcystin). Following centrifugation at 1000 $\times$ *g* for 5 min, the supernatant was collected (fraction I), and pellets were washed with the same buffer. The wash was collected as before (fraction II), and the nuclear pellets were further extracted for 40 min on ice with 150 μl of fractionation buffer containing 0.5% Nonidet P-40. The extracts were clarified by centrifugation at 16,000 $\times$ *g* for 15 min (fraction III). The pellets were finally lysed in SDS-PAGE sample buffer and boiled for 5 min (fraction IV). Equal aliquots of each fraction, derived from equivalent cell numbers, were separated on 8% SDS-PAGE gels and blotted onto polyvinylidene difluoride membranes (Hybond-P; Amersham Pharmacia Biotech). Equal loading of fractions from treated and untreated samples was verified by staining the membranes with Ponceau S (Sigma). Membranes were blocked for 1 h in 5% dry milk in Tris-buffered saline containing 0.1% Tween 20 (T-TBS) and incubated for 1 h with primary antibody diluted in T-TBS containing 1% bovine serum albumin. After three washes with T-TBS, membranes were incubated for 1 h with secondary antibodies in T-TBS containing 5% dry milk. Immunoblots were visualized by enhanced chemiluminescence (Super Signal; Pierce).

In Situ Detergent Extraction and Immunofluorescence—HeLa cells grown on 22-mm^2 glass coverslips to about 70% confluence were untreated or treated with NCS. Unless otherwise noted, the NCS was present in the growth medium throughout the experiment. At the indicated time points, cell extraction was carried out *in situ* by incubating the coverslips in fractionation buffer (described above) containing 0.5% Nonidet P-40 for 20 min on ice. The buffer was removed, and the procedure was repeated for two additional incubations on ice, of 10 and 5 min. Cells were fixed in 4% paraformaldehyde for 10 min at 4 °C, followed by a 10-min incubation with 0.5% Triton X-100. After each step, the coverslips were rinsed three times with PBS. Intact cells (not extracted with Nonidet P-40) were fixed as described above. Coverslips were blocked for 15 min with 1% bovine serum albumin and 10% normal donkey serum in PBS. Primary antibodies were diluted in Primary Antibody Dilution Buffer (Biomeda Corp., Foster City, CA). Cells were incubated with primary antibody for 15 h at 4 °C, washed three times with PBS, and incubated with secondary antibody for 0.5 h at room temperature. Coverslips were washed three times in PBS and mounted using GelMount (Biomeda Corp.). All fluorescence images were obtained using a 410 Carl Zeiss confocal laser-scanning microscope (CLSM) at the following configuration: 25-milliwatt krypton/argon (488, 568 nm) laser lines. Images of the same antibody staining were obtained using the same CLSM parameters (brightness, contrast, pinhall, etc.).

Image Processing and Data Analysis—In order to increase image resolution, all images were processed by the application of deconvolution algorithms, using the maximum likelihood estimation with Huygens2 (Bitplane, Zurich, Switzerland) (21). Deconvolution was carried out on a UNIX-based Onyx work station (Silicon Graphics; Mountain View, CA). Colocalization analysis was performed on a gallery that included all of the treated cells using the Zeiss colocalization function. To quantify and compare the relative amount of retained ATM and γ-H2AX, we used the percentage of positive area (PPA) image analysis procedure (22). Briefly, PPA was calculated as a ratio of the positive stained area to the total cellular area. The positive stained area was determined by measuring the fluorescence intensity of the image above a certain cut-off value that was determined based on the fluorescence intensity histogram for each antibody staining. Total cellular area was determined by measuring the fluorescence intensity above the surrounding background of the image, and it depicts the cellular autofluorescence. The statistical significance was calculated using regression analysis and the Student *t* test in Microsoft Excel (Microsoft, Redmond, WA).

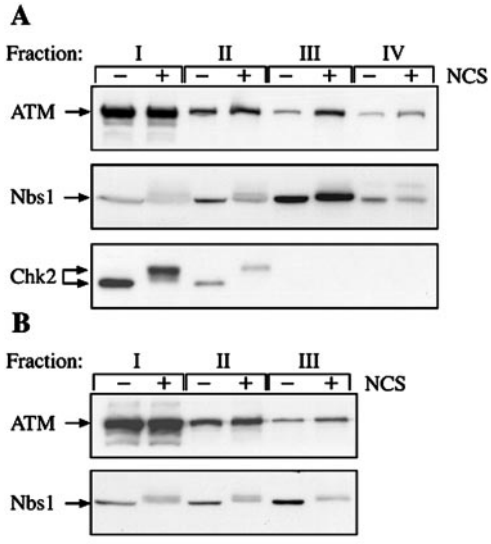

FIG. 1. **A subset of the ATM pool is converted to an extraction-resistant form after DSB induction.** HeLa cells (*A*) or human lymphoblastoid cells, C3ABR (*B*), were left untreated (−) or treated with 200 ng/ml NCS (+). One hour later, cells were harvested and fractionated with Nonidet P-40 as described under "Experimental Procedures." Aliquots equivalent to one-fifth volume of each fraction were separated on 8% SDS-PAGE gels and immunoblotted for ATM and Nbs1 or were run on long 10% gels in order to detect the forms of Chk2.

RESULTS

A Fraction of ATM Becomes Resistant to Detergent Extraction after Radiomimetic Treatment—We designed a cellular fractionation procedure based on successive detergent extractions, aimed at removing loosely bound proteins (described under "Experimental Procedures"). Cells were briefly extracted with 0.2% Nonidet P-40- containing buffer, and the clarified cell extract was collected (fraction I). The cell pellet was washed once in the same buffer (fraction II). A longer extraction with 0.5% Nonidet P-40 was carried out on the remaining pellet (fraction III). Finally, the insoluble remains were boiled in electrophoresis sample buffer (fraction IV). Immunoblot analysis following SDS-PAGE of cell-equivalent aliquots of the four fractions (Fig. 1*A*) showed that the vast majority of the ATM pool was released at the early extraction steps (I and II). Further extraction after longer incubation with detergent (fractions III and IV) showed that only a small amount of ATM was left after the first two fractionation stages of untreated cells.

In cells treated with NCS prior to fractionation, the amount of ATM in the extraction-resistant fractions (III and IV) was considerably higher (about 3–4-fold) than in the equivalent fractions of untreated cells (Fig. 1*A*), and a slight difference was already evident in fraction II. Quantitative analysis of the

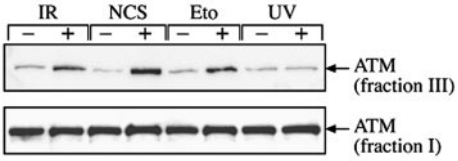

FIG. 2. **DSB-generating agents induce ATM retention.** HeLa cells were mock-treated (−) or exposed to 10 grays of IR, 200 ng/ml NCS, 50 μM etoposide, or 50 J/m^2 of UV-C. One hour later, the cells were fractionated and analyzed as described under "Experimental Procedures." Aliquots of one-fifth volume of fraction III samples and one-fifteenth volume of fraction I were separated on 8% SDS-PAGE and immunoblotted for ATM.

immunoblot demonstrated that about 20% of the ATM pool was retained in NCS-treated cells. Similar results were obtained when Triton X-100 was used instead of Nonidet P-40 or when the longer extraction (stages III and IV) was replaced by complete lysis in radioimmune precipitation buffer (data not shown). Retention of ATM after NCS treatment was also observed in human lymphoblasts (Fig. 1*B*). These results indicate that after induction of DNA damage, a subset of ATM molecules becomes more resistant to detergent extraction, suggesting that ATM is retained due to a tighter association with subnuclear components.

The fractions analyzed in Fig. 1, *A* and *B*, were subjected to immunoblotting for other proteins involved in DSB repair. In each of the fractions, the relative amounts of Ku70, Ku80, DNA-PKcs, BLM, Rad50, and Mre11 were the same for NCS-treated and untreated cells (data not shown). When we used an antibody against Nbs1, a known substrate of ATM, slower migrating bands of Nbs1 appeared in fractions I and II in NCS-treated cells (Fig. 1, *A* and *B*). These bands had previously been shown to represent the phosphorylated forms of Nbs1 (23, 24). Enrichment of a slow migrating form was seen in the extraction-resistant fraction (III and IV) of NCS-treated cells, concomitant with ATM retention (Fig. 1, *A* and *B*). Another substrate of ATM is the checkpoint kinase Chk2/hCds1 (27–29). In contrast to Nbs1 and the other DNA repair proteins mentioned above, neither the basal nor the phosphorylated form of Chk2 could be detected in fractions III or IV of NCS-treated or untreated cells (Fig. 1*A*). This observation indicates that all of Chk2 is readily extracted, in agreement with its role in the transduction of the signal rather than in detection or repair of the damage itself.

ATM Retention Is Specific to DSB-inducing Agents—ATM is activated by agents that generate DSBs, such as IR (9), the radiomimetic drug NCS (10), and the topoisomerase II inhibitor, etoposide.[2] Other genotoxic agents such as UV light, which induces primarily pyrimidine dimers, do not enhance ATM activity (9). In agreement with this, ATM was found to mediate cellular responses to DSB-inducing agents but not other types of DNA-damaging agents (reviewed in Refs. 1 and 2).

We studied retention of ATM following treatment of HeLa cells with IR, NCS, etoposide, and UV-C light. In correlation with ATM activation by these agents, retention of ATM in fraction III was observed only in cells treated with DSB-inducing agents but not after UV irradiation, while there was no detectable change in the amount of loosely bound ATM in fraction I (Fig. 2). These observations indicate that nuclear retention of ATM is induced specifically by agents that generate DNA DSBs.

Time Course and Dose Dependence of ATM Retention—Time course analysis of the extraction-resistant fraction (III) indicated that ATM was retained at the earliest time point examined, 3 min after the addition of NCS to HeLa cells (Fig. 3*A*). No change could be observed in the amount of the loosely bound and major portion of the cellular ATM, detected in fraction I.

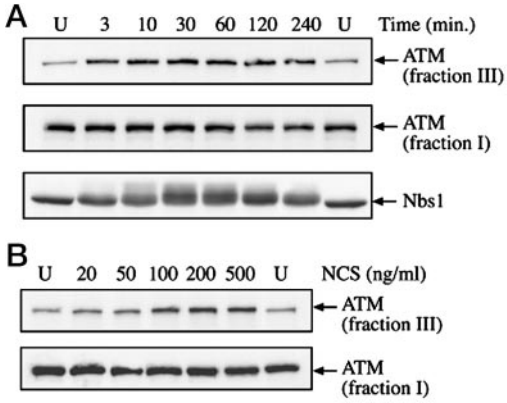

FIG. 3. **Kinetics and dose response of ATM retention.** *A*, HeLa cells were left untreated (*U*) or were treated with 200 ng/ml NCS. At the indicated time points, cells were fractionated with Nonidet P-40 and analyzed as described for Fig. 2. Aliquots of fractions III and fraction I were immunoblotted for ATM, and aliquots of fraction I were also immunoblotted for Nbs1. *B*, HeLa cells were left untreated (*U*) or treated with the indicated concentrations of NCS. After 10 min, cells were fractionated and analyzed as described above.

Notably, the kinetics of Nbs1 phosphorylation was slower than that of ATM retention (Fig. 3*A*).

We next examined the dose dependence of ATM retention by detergent fractionation of HeLa cells at 10 min following exposure to increasing concentrations of NCS. As before, no NCS-induced changes could be observed in the loosely bound ATM that was extracted in fraction I. ATM retention (fraction III) was barely noticed at NCS doses of 20 and 50 ng/ml, but it increased proportionally with higher doses of 100–500 ng/ml (Fig. 3*B*).

ATM Retention Is Not Inhibited by Wortmannin—The antifungal agent wortmannin, a strong inhibitor of ATM (31), was used to investigate whether the kinase activity of ATM is required for its damage-induced nuclear retention. As expected, ATM-mediated phosphorylation of Nbs1 was inhibited by wortmannin at doses higher than 20 μM (Fig. 4). However, this agent had no effect on ATM retention at concentrations of up to 100 μM (Fig. 4). Our results indicate that ATM kinase activity in general, and its autophosphorylation in particular, are not needed for its nuclear retention.

ATM Is Retained in Nuclear Aggregates after NCS Treatment—In order to visualize the retained ATM by immunofluorescence, we adapted a protocol for *in situ* detergent extraction of attached cells (see "Experimental Procedures"). In nonextracted cells, ATM was visible in the nuclei of untreated or NCS-treated cells, and no major NCS-induced alterations in the nuclear distribution of ATM could be detected (Fig. 5, *A* and *B*, *top panels*). Under these conditions, ATM showed diffuse nuclear staining with the exception of the nucleoli that were not stained. However, ATM was lost from the nuclei of untreated HeLa cells after extraction with Nonidet P-40 but was retained in extraction-resistant aggregates in NCS-treated cells (Fig. 5, *A* and *B*, *bottom panels*), in agreement with the results of the biochemical fractionation presented above. Thus, the removal of nucleoplasmic or loosely bound proteins, including the nonretained ATM, enabled clear detection of retained ATM in NCS-treated cells.

Unexpectedly, the overall intensity of ATM staining in NCS-treated cells was roughly similar with or without *in situ* detergent extraction (compare the *top* and *bottom panels* in Fig. 5, *A* and *B*). This observation does not agree with the results of the biochemical analysis presented above, which showed that only about 20% of the ATM pool was retained after detergent fractionation of NCS-treated cells (Fig. 1*A*). This apparent discrep-

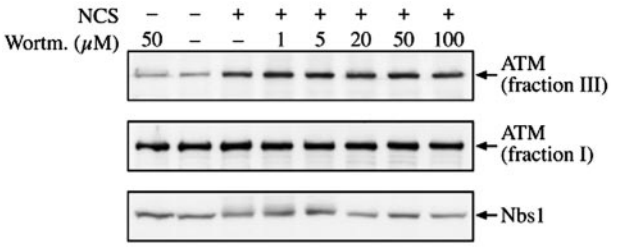

FIG. 4. **Wortmannin does not affect ATM retention in response to NCS treatment.** HeLa cells were exposed to the indicated concentrations of wortmannin 1 h prior to the addition of 200 ng/ml NCS. Cells were harvested 30 min later, fractionated, and analyzed as described for Fig. 2. Aliquots of fraction III and fraction I were immunoblotted for ATM, and aliquots of fraction I were also immunoblotted for Nbs1.

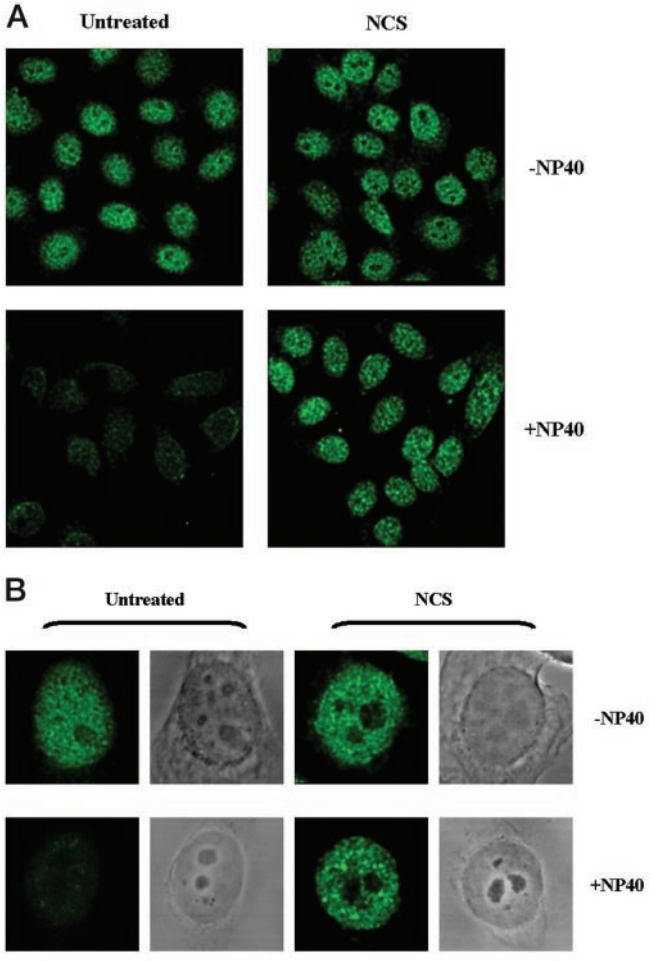

FIG. 5. ***In situ* detergent extraction reveals nuclear retention of ATM following induction of DSBs.** HeLa cells were untreated or were exposed to 200 ng/ml NCS. After 30 min, the cells were extracted *in situ* with the Nonidet P-40 detergent (*+NP40*) or not fractionated (*−NP40*). Cells were stained with a monoclonal anti-ATM antibody. Images were visualized with a CLSM and subjected to image analysis as described under "Experimental Procedures." *A*, magnification × 600. *B*, magnification × 2000. *Images* in the *right panels*, obtained by phase contrast, clearly show that only the nuclei remain after the *in situ* cellular extraction with Nonidet P-40.

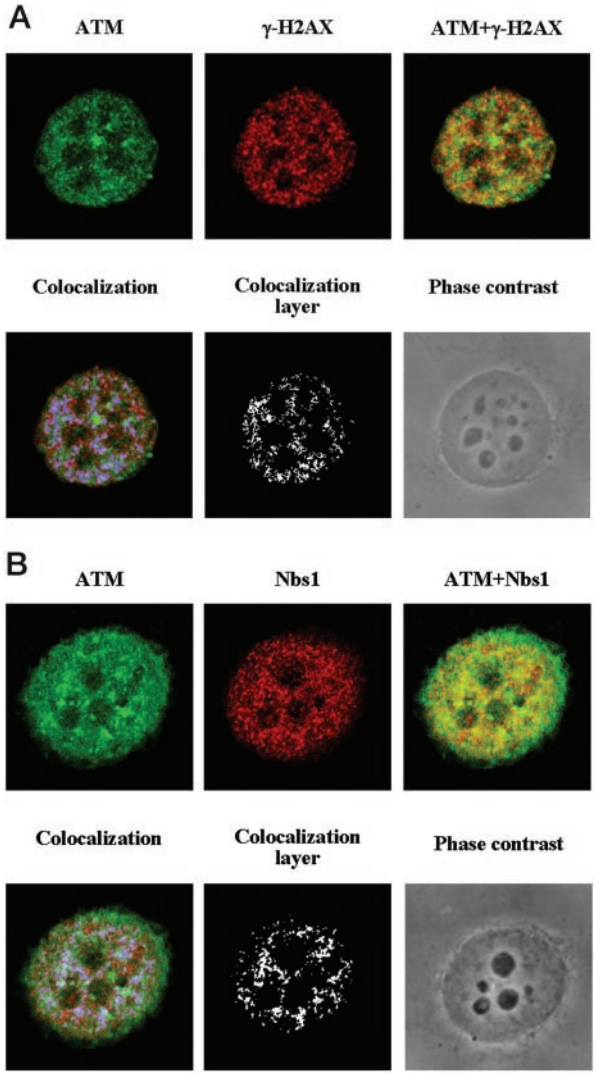

FIG. 6. **Retained ATM colocalizes with γ-H2AX and Nbs1 foci.** *A*, HeLa cells were exposed to 200 ng/ml NCS. After 30 min, the cells were fractionated *in situ* with Nonidet P-40. Cells were co-stained with anti-ATM (*green*) and anti-γ-H2AX (*red*) antibodies. Images obtained with CLSM were subjected to image analysis. The *red* and *green images* were merged (*ATM + γ-H2AX*) and subjected to colocalization analysis, as described under "Experimental Procedures." The colocalization layer was overlaid on the merged image as a *blue* layer (*Colocalization*). Phase contrast was used to visualize the *in situ* fractionated cells (magnification × 2000). *B*, HeLa cells were treated as described for *A* and co-stained with anti-ATM (*green*) and anti-Nbs1 (*red*). Images were analyzed for colocalization as described for *A*.

ancy could be attributed to enhanced accessibility of ATM to the antibody following *in situ* extraction with Nonidet P-40, perhaps due to exposure of relevant epitopes on the ATM protein.

Retained ATM Associates with Sites of Double Strand Breaks—In order to further characterize the sites of ATM retention after DNA damage, we used an antibody specific for γ-H2AX, the phosphorylated form of histone H2AX on serine 139. Foci of γ-H2AX are formed specifically at sites of DNA DSBs, as early as 1 min after infliction of damage (20). Colocalization of some of the extraction-resistant ATM aggregates with foci of γ-H2AX (Fig. 6*A*) indicated that part of the retained ATM is found at sites of DSBs. This notion was further supported by colocalization of retained ATM with Nbs1 (Fig. 6*B*), since the Nbs1-Mre11-Rad50 complex was also shown to accumulate at sites of DSBs (18, 19) and can be detected by *in situ* extraction at early time points after exposure to IR (30).

Time Course and Dose Dependence of ATM Retention Visualized by Immunofluorescence—Extraction-resistant aggregates of ATM, visualized by *in situ* extraction followed by immunostaining, became more abundant with increasing NCS doses (Fig. 7*A*). The number of γ-H2AX foci also increased with increasing levels of DNA damage, in agreement with previous observations (20), and these colocalized with the retained ATM (Fig. 7*A*). The dose dependence of the retained ATM was quan-

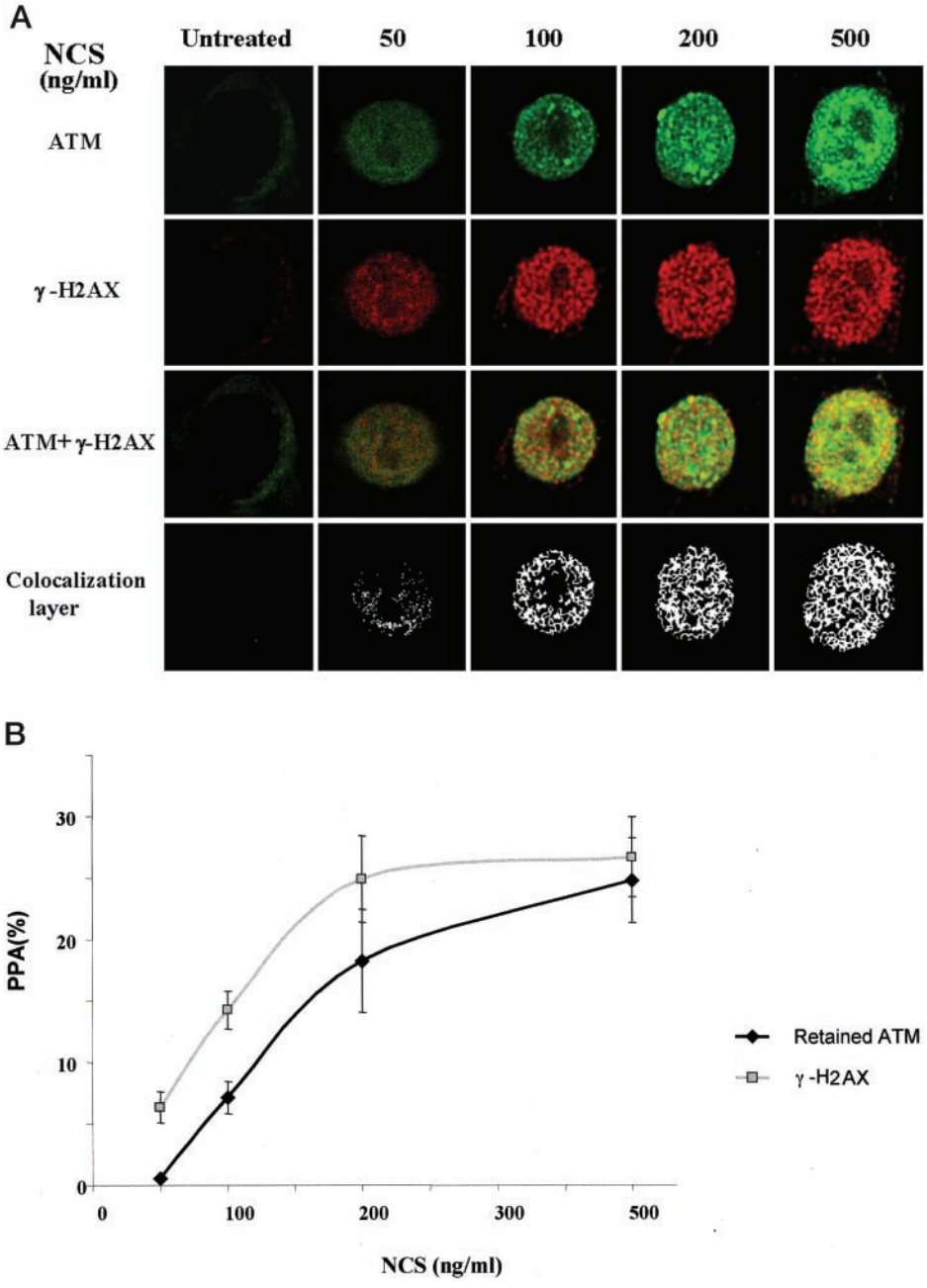

FIG. 7. **Dose response of ATM retention visualized by immunofluorescence.** HeLa cells were left untreated or were treated with the indicated concentrations of NCS. After 30 min, cells were extracted *in situ*, co-stained with anti-ATM (*green*) and anti-γ-H2AX (*red*) antibodies, imaged by CLSM, and subjected to image analysis. *A*, the *red* and *green* images were merged (*ATM + γ-H2AX*) and subjected to colocalization analysis as described in the legend to Fig. 6 (magnification × 2000). *B*, the relative levels of retained ATM and γ-H2AX were calculated using PPA analysis as described under "Experimental Procedures." The *graph* displays the calculated mean and S.D. of PPA for each NCS dose ($n = 16$ independent cells) ($p < 0.001$).

tified by calculating the amount of ATM staining as PPA, as described under "Experimental Procedures." The results of this analysis (Fig. 7*B*) show that the amount of ATM retained after detergent extraction and the amount of γ-H2AX increase proportionally to the concentration of NCS up to about 200 ng/ml, after which both level off. Regression analysis of the PPA showed that the curves fit a natural logarithmic pattern (γ-H2AX: $y = 9.1989\text{Ln}(x) - 28.029$, $R^2 = 0.9029$; ATM: $y = 10.895\text{Ln}(x) - 41.857$, $R^2 = 0.9769$).

In order to follow the kinetics of the appearance and dissolution of retained ATM aggregates, HeLa cells were exposed to 200 ng/ml of NCS for 10 min. The formation of extraction-resistant ATM aggregates increased by 30-fold 30 min following treatment ($p < 0.001$; Fig. 8, *A* and *B*). Their levels decreased dramatically 60 min after treatment and plateaued at low levels by 3 h. Regression analysis of the PPA showed that the curves have a parabolic shape (γ-H2AX: $y = -0.0254x^2 + 1.6246x + 0.2574$, $R^2 = 0.9989$; ATM: $y = -0.0314x^2 + 2.0329x$, $R^2 = 0.9982$).

This kinetics is in complete correlation with the appearance and dissolution of γ-H2AX foci in the same cells (Fig. 8, *A* and *B*). These observations suggest that ATM retention and H2AX phosphorylation occur concomitantly, very rapidly after damage infliction, and decrease at the same rate thereafter.

DISCUSSION

ATM plays a crucial role in the early and rapid activation of numerous responses necessary for cellular survival and preservation of genomic integrity following DSB induction. Extensive studies have recently revealed many of the players in the network of signaling pathways controlled by ATM (reviewed in Ref. 5). However, understanding its mechanism of action in response to DSBs has been hindered by the inability to detect changes in the abundance or nuclear distribution of ATM following DNA damage (11–14).

Using detergent extraction to remove loosely bound ATM, followed by immunoblotting and immunostaining, we obtained evidence of the dynamics in ATM subnuclear associations fol-

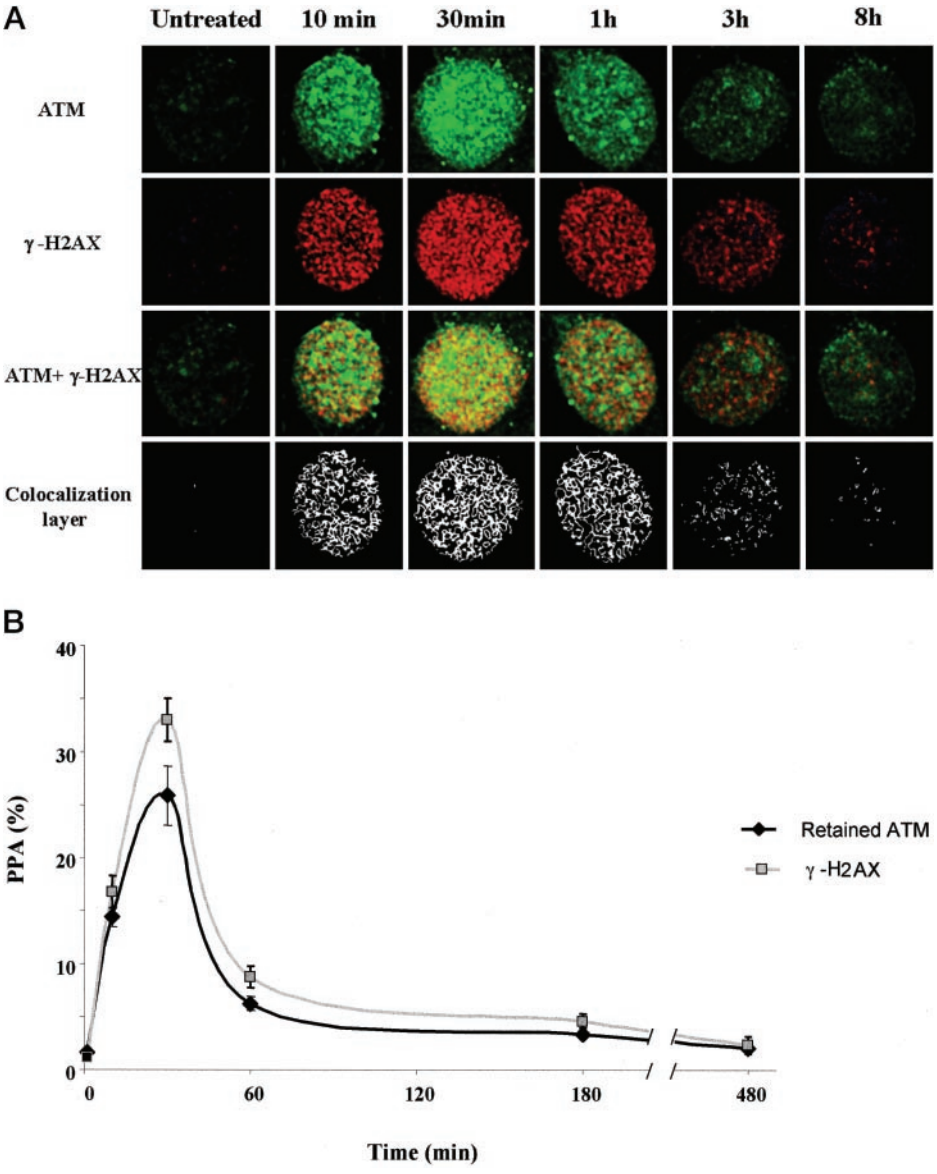

FIG. 8. **Kinetics of ATM retention visualized by immunofluorescence.** HeLa cells were left untreated or were exposed to 200 ng/ml NCS. The drug was removed after 10 min by replacing it with the original growth medium. Cells were extracted *in situ* at the indicated time points, co-stained with anti-ATM (*green*) and anti-γ-H2AX (*red*) antibodies, and analyzed as described for Fig. 7. *A*, the *red* and *green images* were merged (*ATM + γ-H2AX*) and subjected to colocalization analysis as described for Fig. 6 (magnification × 2000). *B*, the relative levels of retained ATM and γ-H2AX at the various time points were calculated using PPA analysis as described under "Experimental Procedures." The *graph* displays the calculated mean and S.D. of PPA for each time point ($n = 16$ independent cells) ($p < 0.001$).

lowing DNA damage. Our observations suggest that while most of the ATM is loosely tethered to the nucleus, a subset of the ATM molecules becomes resistant to extraction immediately after induction of DSBs, probably due to their tighter association with sites of damage in the chromatin.

Gately *et al.* (14) reported that some of the ATM associates with chromatin and the nuclear matrix, but they observed no alterations in the associated fraction of ATM after IR treatment. The discrepancy between their and our results might stem from the different methods used for subcellular fractionation. In addition, they analyzed the ATM in each fraction by immunoprecipitation followed by immunoblotting, whereas we employed direct immunoblotting and immunostaining.

Treatment of cells with wortmannin, an inhibitor of ATM and its relatives, the protein kinases ATR and DNA-PK (31) did not prevent NCS-induced retention of ATM. Thus, DSB-induced retention of ATM does not appear to involve ATM autophosphorylation or the phosphorylation of other proteins by these kinases.

Visualization of retained ATM following DNA damage shows ATM staining as aggregates rather than foci. We cannot determine at this point whether these aggregates result from migration of nucleoplasmic ATM to sites of damage or from enhancement of a weak basal association of ATM with the chromatin and/or other subnuclear compartments.

In situ fractionation was recently used to detect early nuclear retention of the Mre11-Rad50-Nbs1 complex in small granular foci (30). DNA damage-induced conversion to an extraction-resistant form was also reported for hRad9, another protein implicated in the early damage-sensing response (32).

Several proteins involved in DNA repair are recruited and accumulate in nuclear foci after double strand DNA breakage, in accordance with their active role in the repair of damage. These include the Rad51 protein (33), the BRCA1 protein (34), and the Mre11-Rad50-Nbs1 complex (18, 19). Phosphorylation of histone H2AX on serine 139 and foci formation of the phosphorylated form, γ-H2AX, occur with very rapid kinetics. Rogakou *et al.* (20) reported that within seconds of damage infliction, H2AX molecules are phosphorylated en mass at sites of DSBs, and this is visualized as foci of γ-H2AX. A recent study suggested that H2AX phosphorylation and foci formation precede and initiate recruitment of repair factors to nuclear foci after DNA damage (35).

ATM retention, like H2AX phosphorylation and foci formation, takes place at a rapid kinetics. We identified a remarkable correlation between the kinetics of appearance and dissolution of retained ATM and γ-H2AX, supporting our contention that there is a tight linkage between the induction of DSBs and

ATM retention. Our observation that some but not all of the retained ATM is colocalized with γ-H2AX foci suggests that only part of the ATM molecules that increased their association with some nuclear components are bound to sites of DSBs. Thus, unlike the proteins that have an active role in the repair of the DNA breaks and accumulate en mass as foci at DSBs, only a subset of the ATM pool appears to rapidly associate with nuclear components, such as the chromatin and nuclear matrix, and can be found at sites of DSBs. These observations are in agreement with its role in damage surveillance and detection rather than in repair *per se*.

Taken together, our observations indicate that while most of the cellular ATM is loosely tethered to the nucleus, a subset of ATM is rapidly retained, and some of it can be found at sites of DSBs. By anchoring to sites of damage in the chromatin, this fraction of the ATM pool might be the one directly involved in transducing the signal to downstream pathways. These observations underscore the role of ATM in DNA damage surveillance and early detection of DNA DSBs, followed by a rapid transduction of the signal to downstream pathways.

Acknowledgments—We thank Tamar Uziel and Yuval Landau for help and valuable advice, Dr. Martin Lavin for a cell line, and Drs. William Bonner, Steve Elledge, and Eva Lee for antibodies.

REFERENCES

1. Rotman, G., and Shiloh, Y. (1999) *Oncogene* **18,** 6135–6144
2. Shiloh, Y. (2001) *Cold Spring Harbor Symp. Quant. Biol.* **65,** 527–533
3. Lavin, M. F., and Shiloh, Y. (1997) *Annu. Rev. Immunol.* **15,** 177–202
4. Lavin, M. F., and Khanna, K. K. (1999) *Int. J. Radiat. Biol.* **75,** 1201–1214
5. Shiloh, Y., and Kastan, M. B. (2001) *Adv. Cancer Res.* **83,** 210–253
6. Petrini, J. H. (1999) *Am. J. Hum. Genet.* **64,** 1264–1269
7. Wang, J. Y. J. (2000) *Nature* **405,** 404–405
8. Michelson, R. J., and Weinert, T. (2000) *BioEssays* **22,** 966–969
9. Canman, C. E., Lim, D-S., Cimprich, K. A., Taya, Y., Tamai, K., Sakaguchi, K. Appella, E., Kastan, M. B., and Siliciano, J. D. (1998) *Science* **281,** 1677–1679
10. Banin, S., Moyal, L., Shieh, S.-Y., Taya, Y., Anderson, C. W., Chessa, L., Smorodinsky, N. I., Prives, C., Reiss, Y., Shiloh, Y., and Ziv, Y. (1998) *Science* **281,** 1674–1677
11. Lakin, N. D., Weber, P., Stankovic, T., Rottinghous, S. T., Taylor, A. M. R., and Jackson, S. P. (1996) *Oncogene* **13,** 2707–2716
12. Brown, K. D., Ziv, Y., Sadanandan, S. N., Chessa, L., Collins, F. S., Shiloh, Y., and Tagle, D. A. (1997) *Proc. Natl. Acad. Sci. U. S. A.* **94,** 1840–1845
13. Watters, D., Khanna, K. K., Beamish, H., Birrell, G., Spring, K., Kedar, P., Gatei, M., Hobson, K., Kozlov, S., Zhang, N., Farrell, A., Ramsay, J., Gatti, R., and Lavin, M. (1997) *Oncogene* **14,** 1911–1921
14. Gately, D. P., Hittle, J. C., Chan, G. K. T., and Yen, T. J. (1998) *Mol. Biol. Cell* **9,** 2361–2374
15. Pandita, T. K., Lieberman, H. B., Lim, D-S, Dhar, S., Zheng, W., Taya, Y., and Kastan, B. M. (2000) *Oncogene* **19,** 1386–1391
16. Smith, G. C. M., Cary, R. B., Lakin, N. D., Hann, B. C., Teo, S-H., Chen, D. J., and Jackson, S. P. (1999) *Proc. Natl. Acad. Sci. U. S. A.* **96,** 11134–11139
17. Suzuki, K., Kodama, S., and Watanabe, M. (1999) *J. Biol. Chem.* **274,** 25571–25575
18. Maser, R. S., Monsen, K. J., Nelms, B. E., and Petrini, J. H. J. (1997) *Mol. Cell. Biol.* **17,** 6087–6096
19. Nelms, B. J., Maser, R. S., McKay, J. F., Lagally, M. G., and Petrini, J. H. J. (1998) *Science* **280,** 590–592
20. Rogakou, E. P., Boon, C., Redon, C., and Bonner, W. M. (1999) *J. Cell Biol.* **146,** 905–915
21. Holmes, T. J. (1992) *J. Opt. Soc. Am. A* **9,** 1052–1061
22. Ronen, D., Alstock, M., Firon, M., Mittelman, L., Sobe, T., Reseau, J. H., Vande Woude, G. F., and Tsarfaty, I. (1999) *Cell Growth Differ.* **10,** 131–140
23. Gatei, M., Young, D., Cerosaletti, K. M., Desai-Mehta, A., Spring, K., Kozlov, S., Lavin, M. F., Gatti, R. A., Concannon, P., and Khanna, K. K. (2000) *Nat. Genet.* **25,** 115–119
24. Lim, D-S., Kim, S-T., Xu, B., Maser, R. S., Lin, J., Petrini, J. H. J., and Kastan, M. B. (2000) *Nature* **404,** 613–617
25. Wu, X., Ranganathan, V., Weisman, D. S., Heine, W. F., Ciccone, D. N., O'Neill, T. B., Crick, K. E., Pierce, K. A., Lane, W. S., Rathbun, G., Livingston, D. M., and Weaver, D. T. (2000) *Nature* **405,** 477–482
26. Zhao, S., Weng, Y-C., Yuan, S-S. F., Lin, Y-T., Hsu, H-C., Lin, S-C. J., Gerbino, E., Song, M-H., Zdzienicka, M. Z., Gatti, R., Shay, J. W., Ziv, Y., Shiloh, Y., and Lee, E. Y-H. P. (2000) *Nature* **405,** 473–477
27. Ahn, J. Y, Schwarz, J. K., Piwnica-Worms, H., and Canman, C. E. (2000) *Cancer Res.* **60,** 5934–5936
28. Matsuoka, S., Rotman, G., Ogawa, A., Shiloh, Y., Tamai, K., and Elledge, S. J. (2000) *Proc. Natl. Acad. Sci. U. S. A.* **97,** 10389–10394
29. Melchionna, R., Chen, X-B., Blasina, A., and McGowan, C. H. (2000) *Nat. Cell Biol.* **2,** 762–765
30. Mirzoeva, O. K., and Petrini, J. H. J. (2001) *Mol. Cell. Biol.* **21,** 281–288
31. Sarkaria, J. N., Tibbets, R. S., Busby, E. C., Kennedy, A. P., Hill, D. E., and Abraham, R. T. (1998) *Cancer Res.* **58,** 4375–4382
32. Burtelow, M. A., Kaufmann, S. H., and Karnitz, L. M. (2000) *J. Biol. Chem.* **275,** 26343–26348
33. Haaf, T., Golub, E., Reddy, G., Radding, C. M., and Ward, D. C. (1995) *Proc. Natl. Acad. Sci. U. S. A.* **92,** 2298–2302
34. Scully, R. S., Chen, J., Ochs, R. L., Keegan, K., Hoekstra, M., Feunteun, J., and Livingston, D. M. (1997) *Cell* **90,** 425–435
35. Paull, T. T., Rogakou, E. P., Yamazaki, V., Kirchgessner, C. U., Gellert, M., and Bonner, W. M. (2000) *Curr. Biol.* **10,** 886–895

Nuclear Retention of ATM at Sites of DNA Double Strand Breaks

Yair Andegeko, Lilach Moyal, Leonid Mittelman, Ilan Tsarfaty, Yosef Shiloh and Galit Rotman

J. Biol. Chem. 2001, 276:38224-38230.
originally published online October 5, 2001
